Supporting Information (SI)

An advanced furoxan-bridged heat-resistant explosive

Chengchuang Li[a], Teng Zhu[a], Jie Tang[a], Caijin Lei[a], Guoyang Yu[c], Yanqiang Yang[c], Hongwei Yang*[a] Chuan Xiao*[b] and Guangbin Cheng*[a]

a. School of Chemistry and Chemical Engineering, Nanjing University of Science and Technology, Xiaolingwei 200, Nanjing, Jiangsu, China.
*Corresponding author E-mail: hyang@mail.njust.edu.cn (H. Yang), gcheng@mail.njust.edu.cn (G. Cheng).
b. China Northern Industries Group Co., Ltd. (NORINCO GROUP), Beijing 100089, P. R. China
*Corresponding author E-mail: 47785121@qq.com (C. Xiao).
c. National Key Laboratory of Shock Wave and Detonation Physics, Institute of Fluid Physics, China Academy of Engineering Physics, No.64 Mianshan Road, Mianyang, Sichuan, China.

Table of Contents

1. Experimental sections

General methods

^{1}H and ^{13}C NMR spectra were recorded on 500 MHz (Bruker AVANCE 500) nuclear magnetic resonance spectrometers operating at 500 and 126 MHz, respectively, by using DMSO-d6 as the solvent and locking solvent unless otherwise stated. Chemical shifts in ^{1}H and ^{13}C NMR spectra are reported relative to DMSO. DSC was performed in closed Al containers with a nitrogen flow of 30 mL min^{-1} on an STD-Q600 instrument. Infrared (IR) spectra were recorded on a Perkin-Elmer Spectrum BX FT-IR equipped with an ATR unit at 25 °C. Impact sensitivity and friction sensitivity of samples are measured by using the standard BAM methods. Densities were determined at 25 °C by employing a Micromeritics AccuPyc II 1345 gas pycnometer. Elemental analyses of C/H/N were performed on a Vario EL III Analyzer. X-ray intensity data were collected on a Bruker D8 VENTURE PHOTON II system equipped with an Incoatecius 3.0 Microfocus sealed tube. The structures were solved and refined using Bruker SHELXTL Software Package. The data were refined against F2. All non-hydrogen atoms were refined anisotropically. Hydrogen atoms were fixed to their parent atoms using a riding model and refined isotropically. The thermal sensitivity of sample was measured to evaluate its thermal resistance by an OZM Instruments AET402 automatic explosion temperature tester.

Synthesis

2-(4-amino-3-nitropyrazolo[5,1-c][1,2,4]triazin-7-yl)acetic acid (**2**):

To a mixture of 2-(3-amino-1*H*-pyrazol-5-yl)acetic acid (**1**) (2.28 g, 20 mmol) was suspended in 20.0 ml water and 5.0 ml concentrated hydrochloric acid. A solution of sodium nitrite (1.80 g, 24.0 mmol) in distilled water (8 ml) was added dropwise at -5 ◦C. After the addition, the reaction mixture was stirred at this temperature for 10 h. To this solution the solution of nitroacetonitrile (2.50 g, 30.0 mmol) and sodium hydroxide (1.60 g, 40.0 mmol) in 20 ml water was added dropwise. The mixture was allowed to warm to room temperature (20 °C) and stirred for 24 h. The precipitate was filtered and washed with water, then dried in the air to yield 4.20 g (87%) of compound **2**. The infrared spectroscopy (IR), multinuclear NMR (^{1}H, ^{13}C) spectroscopy and elemental analysis can be find in reference [12].

3,4-bis(4-amino-3,8-dinitropyrazolo[5,1-c][1,2,4]triazin-7-yl)-1,2,5-oxadiazole 2-oxide (**OTF**):

100% nitric acid (5.0 mL) was added to a mixture of 98% sulfuric acid (5.0 mL) and

trifluoroacetic acid (1.0 mL) at 0 °C. Then, the compound **2** (1.19 g, 5.0 mmol) was added to the reaction mixture in batches. After being stirred for 12 hours at room temperature, the solution was poured into ice. The resulting precipitate was collected by filtration, washed with water, and yielded 2.36 g (89%) of compound **4** as a light-yellow solid. ^{1}H NMR (500 MHz, DMSO-d6): δ = 10.41 (br, NH_2) ppm. ^{13}C NMR (126 MHz, DMSO-d6): δ = 119.48, 120.11, 138.91, 140.96, 143.15, 145.07 ppm. IR (KBr): ṽ 3458.1, 3295.4, 3291.6, 1713.1, 1673.8, 1599.0, 1383.4, 1362.3, 1330.2, 1315.1, 1285.1, 1252.3, 1243.8, 1115.7, 823.8, 799.9, 798.2, 752.0, 745.0, 638.0, 631.2, 548.9, 543.3, 465.3, 458.2, 138.8 cm^{-1}. Elemental analysis for $C_{12}H_4N_{16}O_{10}$ (532.27): calcd C, 27.08; H, 0.76; N, 42.11%. Found: C 27.01, H 0.74, N 42.20%.

2. Quantum chemical computational details

All calculations in this work were performed using Gaussian 09 program package1. Full geometry optimizations were performed to locate all the stationary points, using the B3LYP2 with the def2tzvp3-4 basis, namely B3LYP/def2tzvp. Dispersion corrections were computed with Grimme's D3(BJ) method in optimization5. The intrinsic reaction coordinate (IRC) path was traced to check the energy profiles connecting each transition state to two associated minima of the proposed mechanism6. Harmonic vibrational frequency was performed at the same level to guarantee that there is no imaginary frequency in the molecules, i.e. they locate on the minima of potential energy surface. Convergence parameters of the default threshold were retained (maximum force within 4.5×10−4 Hartrees/Bohr and root mean square (RMS) force within 3.0×10−4 Hartrees/Radian) to obtain the optimized structure. The optimal structure was identified given that all calculations for structural optimization were successfully converged within the convergence threshold of no imaginary frequency, during the process of vibration analysis.

3. Computational details of HOF

Computations were performed by using the Gaussian09 suite of programs.[7] The elementary geometric optimization and the frequency analysis were performed at the level of the Becke three parameter, Lee-Yan-Parr (B3LYP) functional with the 6-

311+G** basis set.[8-10] All of the optimized structures were characterized to be local energy minima on the potential surface without any imaginary frequencies. Atomization energies were calculated by the CBS-4M.[11] All the optimized structures were characterized to be true local energy minima on the potential-energy surface without imaginary frequencies.

The predictions of heats of formation (HOF) of compounds used the hybrid DFTB3LYP methods with the 6-311+G** basis set through designed isodesmic reactions. The isodesmic reaction processes, that is, the number of each kind of formal bond is conserved, were used with the application of the bond separation reaction (BSR) rules. The molecule was broken down into a set of two heavy-atom molecules containing the same component bonds. The isodesmic reactions used to derive the HOF shown in Scheme S1.

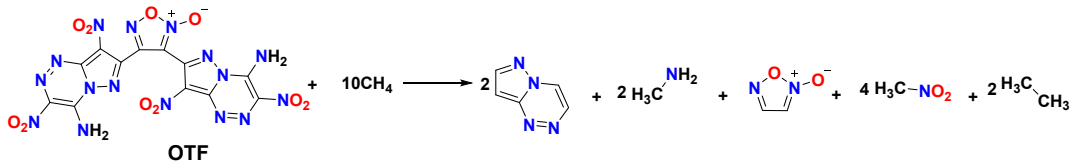

Scheme S1. The isodesmic reactions for calculating heat of formation.

The change of enthalpy for the reactions at 298K can be expressed by Equation (1):

$$\Delta H_{298} = \Sigma\Delta_f H_P - \Sigma\Delta_f H_R \qquad (1)$$

Where $\Sigma\Delta_f H_P$ and $\Sigma\Delta_f H_R$ are the *HOF* of the reactants and products at 298 K, respectively, and ΔH_{298} can be calculated from the following expression in Equation (2):

$$\Delta H_{298} = \Delta E_{298} + \Delta(PV) = \Delta E_0 + \Delta ZPE + \Delta H_T + \Delta nRT \qquad (2)$$

where ΔE_0 is the change in total energy between the products and the reactants at 0 K; ΔZPE is the difference between the zero-point energies (*ZPE*) of the products and the reactants at 0 K; ΔH_T is the thermal correction from 0 to 298 K. The $\Delta(PV)$ value in Equation (2) is the *PV* work term. It equals ΔnRT for the reactions of an ideal gas. For the isodesmic reactions $\Delta n = 0$, so $\Delta(PV) = 0$. On the left side of Equation (2), apart from target compound all the others are called reference compounds. The HOF of reference compounds are available either from experiments or from the high-level computing such as CBS-4M.

4. Crystallographic data

Table S1. Crystallographic data for **OTF**.

Crystal	**OTF**·$CH_3OH·H_2O$	**OTF**·$4CH_3OH$	**OTF**·$1.75C_2H_3N$	**OTF**·$2C_2H_6OS$
CCDC number	2338095	2372336	2372335	2372337
Empirical Formula	$C_{13}H_{11}N_{16}O_{12}$	$C_{16}H_{20}N_{16}O_{14}$	$C_{15.5}H_{9.25}N_{17.75}O_{10}$	$C_{20}H28N_{16}O_{14}S_4$
Formula weight	582.37	660.48	604.16	844.82
Temperature [K]	193.0	198.0	193.0	193.15
Crystal system	triclinic	triclinic	triclinic	monoclinic
Space group	P-1	P-1	P-1	P2/c
a/Å	7.0832(19)	9.2092(11)	6.4781(2)	23.6344(6)
b/Å	11.664(3)	10.8368(13)	13.5834(3)	8.8105(2)
c/Å	13.430 (4)	14.1420(16)	14.1528(4)	18.3794(5)
α/°	98.143(12)	105.307(4)	71.0000(10)	90
β/°	95.040(12)	91.114(4)	81.949(2)	110.3560(10)
γ/°	94.764(12)	99.187(4)	88.8700(10)	90
Cell volume ($Å^3$)	1089.0(5)	1341.0(3)	1165.47(6)	3588.15(16)
Formula Z	2	2	2	4
Density (g cm^{-3})	1.776	1.636	1.722	1.564
μ (mm^{-1})	1.394	0.144	1.289	3.202
F (000)	592.0	680.0	613.0	1744.0
Crystal Size (mm^3)	0.10×0.12×0.14	0.13×0.11×0.1	0.13×0.12×0.11	0.14×0.13×0.1
2θ range for data collection (°)	6.682 to 137.356	3.954 to 50.698	6.672 to 136.15	9.634 to 136.526
Index ranges	-8 ≤ h ≤ 8, -14 ≤ k ≤ 9, -16 ≤ l ≤ 16	-11 ≤ h ≤ 11, -13 ≤ k ≤ 12, -16 ≤ l ≤ 17	-7 ≤ h ≤ 7, -16 ≤ k ≤ 14, -17 ≤ l ≤ 16	-28 ≤ h ≤ 28, -10 ≤ k ≤ 10, -22 ≤ l ≤ 22
Reflections collected	12122	18604	15540	33356
Independent reflections	3915 [R_{int} = 0.0781, R_{sigma} = 0.0699]	4856 [R_{int} = 0.0901, R_{sigma} = 0.0803]	4229 [R_{int} = 0.0620, R_{sigma} = 0.0592]	6567 [R_{int} = 0.0423, R_{sigma} = 0.0301]
Data/restraints/parameters	3915/8/390	4856/112/470	4229/52/437	6567/220/627

Goodness-of-fit on F^2	0.954	1.057	1.053	1.032
Final R indexes [I>=2σ (I)]	R_1 = 0.0597, wR_2 = 0.1494	R_1 = 0.0626, wR_2 = 0.1452	R_1 = 0.0406, wR_2 = 0.1022	R_1 = 0.0423, wR_2 = 0.1088
Final R indexes [all data]	R_1 = 0.1020, wR_2 = 0.1749	R_1 = 0.1079, wR_2 = 0.1751	R_1 = 0.0701, wR_2 = 0.1104	R_1 = 0.0481, wR_2 = 0.1128

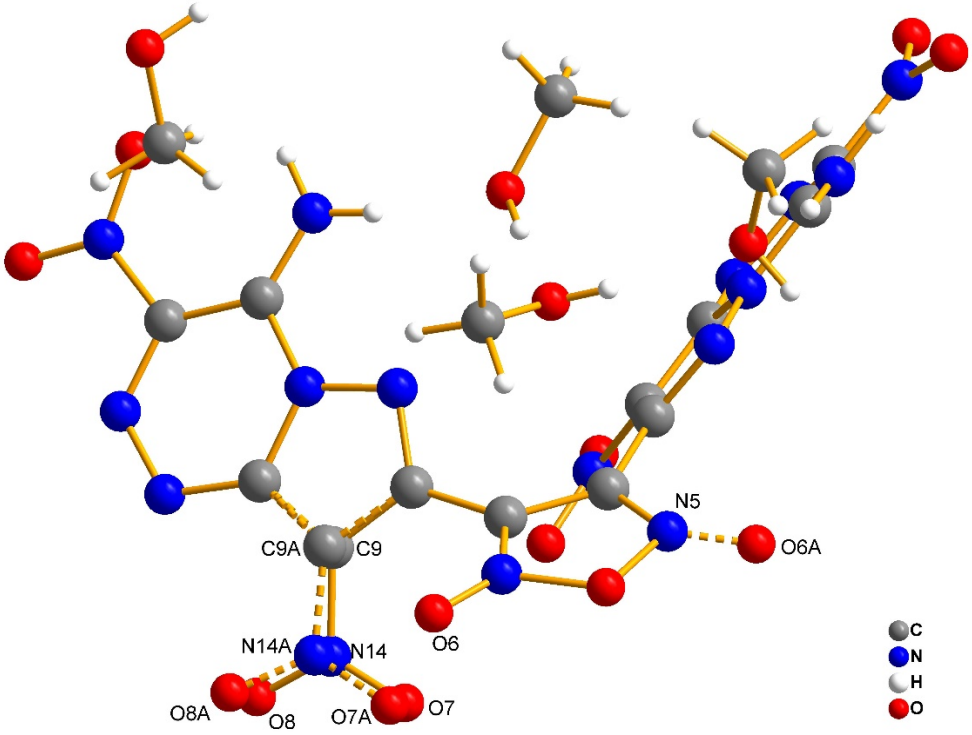

Caution: In **OTF**·4CH_3OH, the residual peak near the N5 is from the disorder of O6 and is not serious. Now it has been refined according to the disorder of O6. The disorder near O7/O8 is due to the disorder of the nitro group， and we have re-established the disorderly model of the nitro group. In the picture, O7A/N14A/O8A is the disorder of the nitro group. Now, the molecular geometric is normal.

In **OTF**·1.75C_2H_3N, due to the severe disorder of the acetonitrile solvent involved in crystallization, restriction commands such as DFIX, SIMU, RIGU, and DANG were used during the analysis.

Table S2. Bond lengths for **OTF**·CH_3OH·H_2O.

Parameter	Bond length (Å)	Parameter	Bond length (Å)
O1-N1	1.233(5)	N9-C7	1.320(5)
O2-N1	1.217(5)	N10-N11	1.367(4)
O3-N7	1.235(6)	N10-C8	1.322(5)
O4-N7	1.210(6)	N11-C10	1.372(5)
O5-N8	1.220(4)	N11-C11	1.364(5)
O5A-N9	1.18(3)	N12-C11	1.407(5)
O6-N9	1.378(5)	N13-C11	1.351(5)
O6-N8	1.433(4)	N13-C11	1.316(5)
O7-N12	1.233(5)	N14-C11	1.331(5)
O8-N12	1.231(5)	N15-C11	1.301(5)
O9-N16	1.213(5)	N16-C11	1.445(5)
O10-N16	1.217(5)	C1-C2	1.427(5)
O12-C13	1.392(7)	C3-C4	1.390(5)
N1-C1	1.459(5)	C4-C5	1.408(5)
N2-C1	1.321(6)	C5-C6	1.452(5)

Table S3. Bond angles for **OTF**·CH_3OH·H_2O.

Atom	Atom	Atom	Angle/°	Atom	Atom	Atom	Angle/°
N8	-O6	-N9	108.2(3)	N1	-C1	-C2	119.4(4)
O1	-N1	-O2	124.0(4)	N2	-C1	-C2	126.3(4)
O2	-N1	-C1	117.4(4)	N1	-C1	-N2	114.3(3)
O1	-N1	-C1	118.6(3)	N4	-C2	-C1	130.5(4)
O4	-N3	-C1	118.7(2)	N4	-C2	-N5	119.8(3)
N3	-N2	-C1	123.8(2)	N5	-C2	-C1	109.7(3)
N2	-N3	-C3	118.1(1)	N3	-C3	-C4	132.6(4)
N6	-N5	-C2	121.8(3)	N3	-C3	-N5	123.2(3)
N6	-N5	-C3	113.9(3)	N5	-C3	-C4	104.2(3)
C2	-N5	-C3	123.1(3)	N7	-C4	-C5	127.1(4)

N5	-N6	-C5	103.9(3)	C3	-C4	-C5	106.6(3)
O4	-N7	-C4	118.8(4)	N7	-C4	-C3	125.7(4)
O3	-N7	-O4	124.7(4)	N6	-C5	-C4	111.4(3)
O3	-N7	-C4	116.5(4)	N6	-C5	-C6	116.8(3)
O8	-N7	-C6	107.3(3)	N8	-C6	-C7	106.6(3)

Table S4. Torsion angles for **OTF**·CH_3OH·H_2O.

Parameter	Bond angles (Å)	Parameter	Bond angles (Å)
O4-N7-C4-C5	17.6(7)	N10-N11-C11-N15	2.2(5)
O4-N7-C4-C3	-153.6(4)	N10-N11-C10-C9	-0.3(4)
O6-N8-C6-C7	176.3(3)	C3-N5-C2-N4	178.5(4)
O5-N8-C6-C5	-178.2(4)	C3- N5-N6-C5	-1.6(4)
O6-N9-C7-C6	176.4(3)	C2- N5-N6-C5	178.0(3)
O6-N9-C7-C8	0.0(4)	N6- N5-C3-N3	179.6(3)
N11-N10-C8-C9	0.4(4)	C3- N5-C2-C1	-2.2(5)
N11-N10-C8-C7	-175.8(3)	N6-N5-C2-C1	178.3(3)

Table S5. Hydrogen bonds for **OTF**·CH_3OH·H_2O.

D-H···A	d(D-H)/ Å	d(H···A)/ Å	d(D···A)/ Å	<(DHA)/ º
N4-H4B···O1	0.8800	2.1200	2.701(5)	123.00
N4-H4B···O9	0.8800	2.5600	3.096(5)	120.00
N4- H4B···O10	0.8800	2.5500	3.296(6)	143.00
O11- H11A···O8	0.8700	2.4300	3.143(5)	140.00
O11- H11A···N13	0.8700	2.1500	2.855(5)	138.00
N15- H15A···N10	0.8800	2.4100	2.743(5)	103.00
N15- H15A··O5	0.8800	2.1300	2.953(5)	155.00
O12- H12···N3	0.8400	2.2300	3.028(5)	159.00

5. Spectrums of compounds

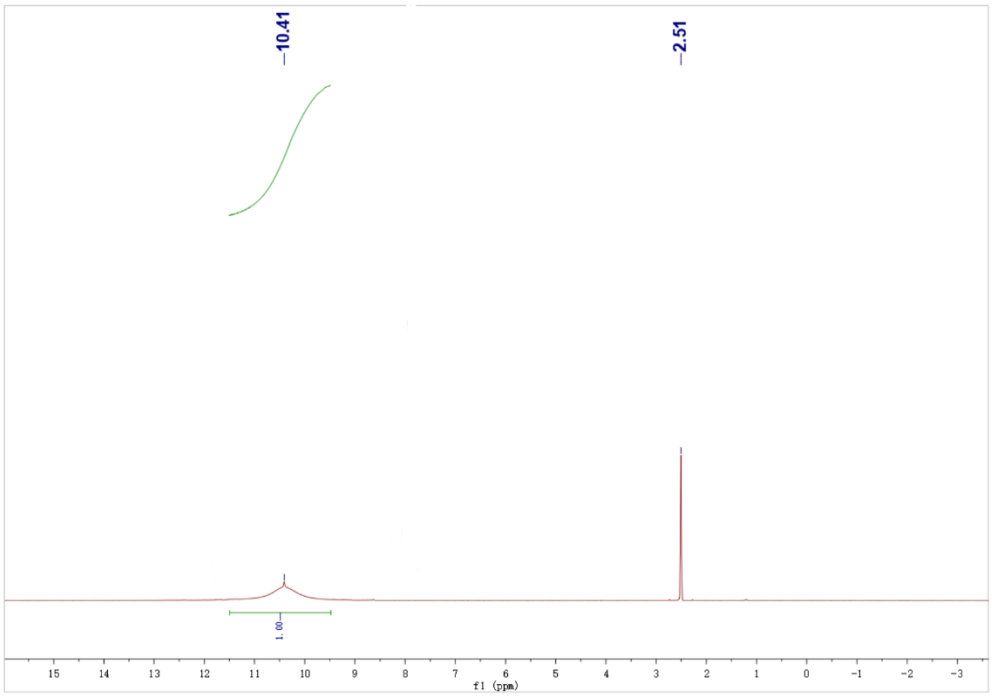

Figure S1. ^{1}H NMR spectra in DMSO-d6 for **OTF**.

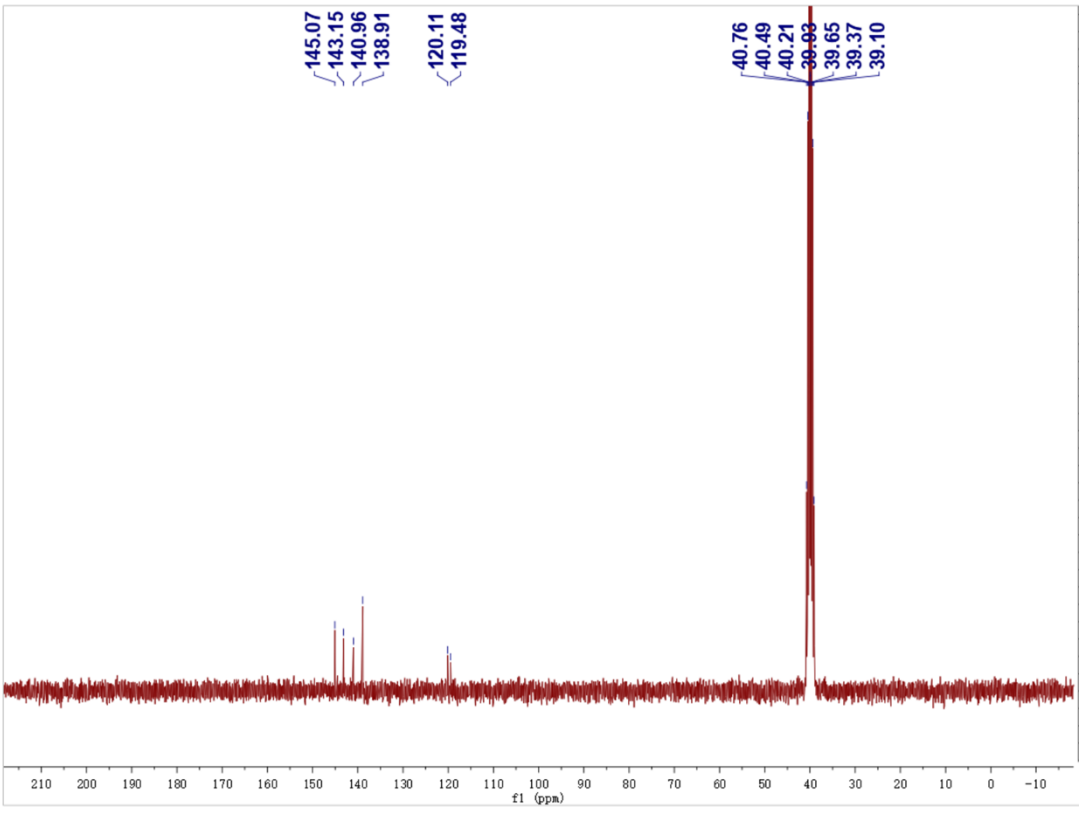

Figure S2. ^{13}C NMR spectra in DMSO-d6 for **OTF**.

6. DSC and TG of compounds

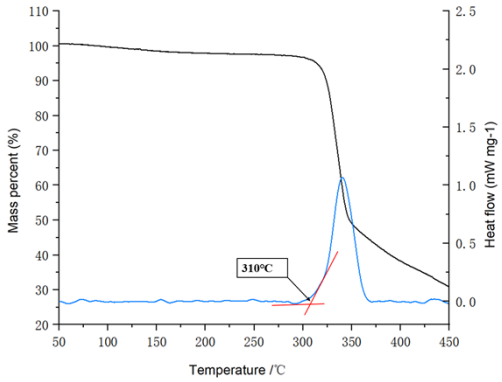

Figure S3 TG and DSC of **OTF** (5K/min).

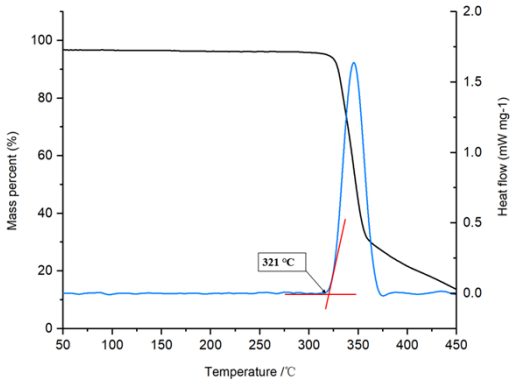

Figure S4 TG and DSC of **OTF** (10K/min).

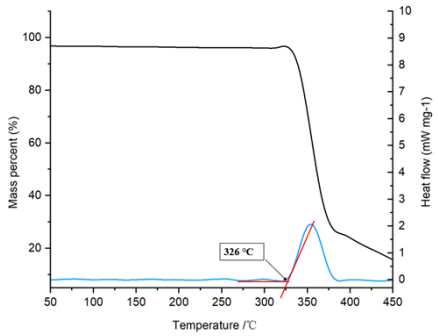

Figure S5 TG and DSC of **OTF** (15K/min).

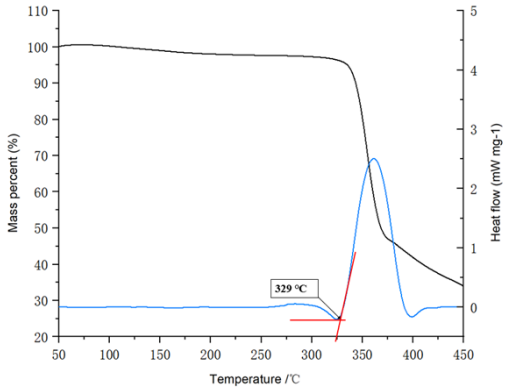

Figure S6 TG and DSC of **OTF** (20K/min).

7. Linear correlation between shock velocity and detonation performance

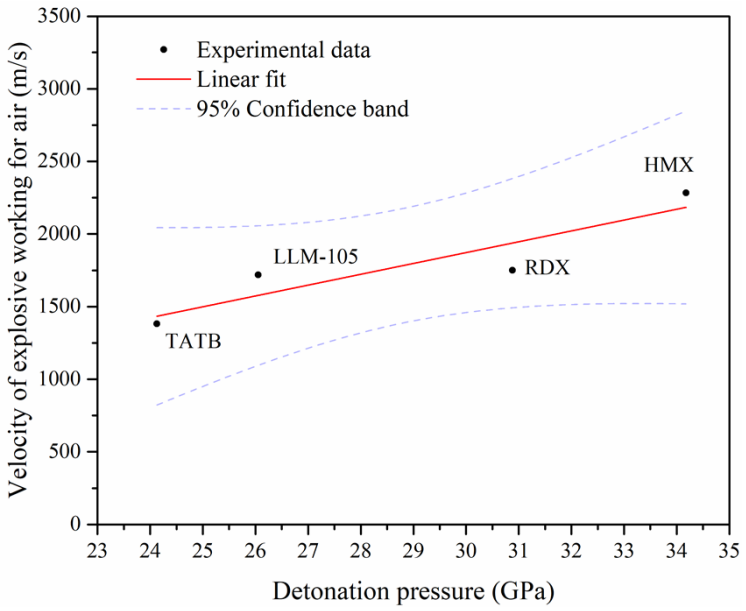

Figure S7 Correlation between the laser-induced air shock velocity and the calculated detonation pressure for conventional energetic materials

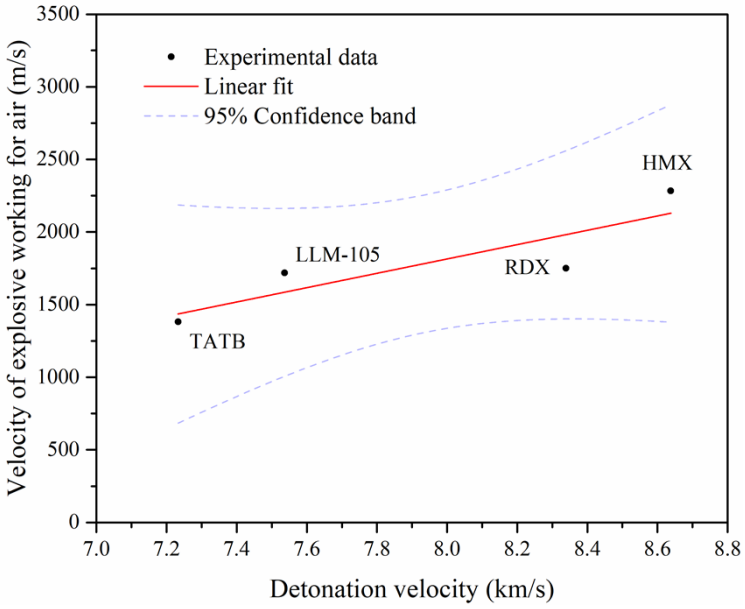

Figure S8 Correlation between the laser-induced air shock velocity and the calculated detonation velocity for conventional energetic materials

8. References

[1] Barone, B. Mennucci, G.A. Petersson, H. Nakatsuji, M. Caricato, X. Li, H.P. Hratchian, A.F. Izmaylov, J. Bloino, G. Zheng, J.L. Sonnenberg, M. Hada, M. Ehara, K. Toyota, R. Fukuda, J. Hasegawa, M. Ishida, T. Nakajima, Y. Honda, O. Kitao, H. Nakai, T. Vreven, J.A. Montgomery, J.J.E. Peralta, F. Ogliaro, M. Bearpark, J.J. Heyd, E. Brothers, K.N. Kudin, V.N. Taroverov, T. Keith, R. Kobayashi, J. Normand, K. Raghavachari, A. Rendell, J.C. Burant, S.S. Iyengar, J. Tomasi, M. Cossi, N. Rega, J.M. Millam, M. Klene, J.E. Knox, J.B. Cross, V. Bakken, C. Adamo, J. Jaramillo, R. Gomperts, R.E. Stratmann, O. Yazyev, A. J. Austin, R. Cammi, C. Pomelli, J. W. Ochterski, R.L. Martin, K. Morokuma, V.G. Zakrzewski, G.A. Voth, P. Salvador, J.J. Dannenberg, S. Dapprich, A.D. Daniels, O. Farkas, J.B. Foresman, J.V. Ortiz, J. Cioslowski, D.J. Fox, Gaussian 09 (Revision D.01), I. Gaussian, Wallingford, CT, 2013.

[2] Krishnan, R.; Binkley, J. S.; Seeger,R.; Pople, J. A., Self-consistent molecular orbital methods. XX. A basis set for correlated wave functions. *J. Chem. Phys.* **1980,** *72* (1), 650-654.

[3] Weigend, F.; Ahlrichs, R., Balanced basis sets of split valences, triple zeta valence

and quadruple zeta valence quality for H to Rn: Design and assessment of accuracy. *Phys Chem Chem Phys* **2005,** *7* (18), 3297-305.

[4] Xu S., He T., Li J., Huang Z., & Hu C., Enantioselective synthesis of D-lactic acid via chemocatalysis using MgO: Experimental and molecular-based rationalization of the triose's reactivity and preliminary insights with raw biomass. *Appl. Catal. B: Environ.* **2021**, 292:120145.

[5] Grimme, S.; Antony, J.; Ehrlich, S.; Krieg, H., A consistent and accurate *ab initio* parametrization of density functional dispersion correction (DFT-D) for the 94 elements H-Pu. *J. Chem. Phys.* **2010,** *132* (15), 154104.

[6] Gonzalez, C.; Schlegel, H. B., An improved algorithm for reaction path following. *J. Chem. Phys.* **1989,** *90* (90), 2154-2161.

[7] M. J. Frisch. Gaussian 09, Revision D. 01 (Gaussian Inc., 2009).

[8] A. D. Becke, *J. Chem. Phys.* **1993**, 98, 5648-5652

[9] P. J. Stephens; F. J. Devlin; C. F. Chabalowski; M. J. Frisch. J. Phys. Chem. **1994**, 98, 11623-11627.

[10] P. C. Hariharan; J. A. Pople, Theor. Chim. Acta. **1973**, 28, 213-222.

[11] J. W. Ochterski; G. A. Petersson; J. A . Montgomery, J. Chem. Phys. **1996**, 104, 2598-2619.

[12] C. Li; T. Zhu; J. Tang; H. Yang; C. Xiao and G. Cheng. Chem. Eng. J, **2024**, 479, 147355.